eCELLS & MATERIALS

OPEN ACCESS

THREE-DIMENSIONAL CULTURE MODEL TO STUDY THE BIOLOGY OF VACUOLATED NOTOCHORDAL CELLS FROM MOUSE NUCLEUS PULPOSUS EXPLANTS

L. Paillat[1], K. Coutant[1,$], M. Dutilleul[1], S. Le Lay[2,#] and A. Camus[1,*]

[1] Nantes Université, Oniris, CHU Nantes, INSERM, Regenerative Medicine and Skeleton, RMeS, UMR 1229, F-4400 Nantes, France

[2] Université Angers, SFR ICAT, F-49000 Angers, France

[$] Present address: Axe Médecine Régénératrice, Centre de Recherche du CHU de Québec-Université Laval, QC, Canada

[#] Present address: Université de Nantes, CNRS, INSERM, l'institut du thorax, F-44000 Nantes, France

Abstract

Intervertebral disc degeneration (IDD) involves cellular changes in the nucleus pulposus (NP) characterised by a decline of the large vacuolated notochordal cells (vNCs) and a rise of smaller vacuole-free mature chondrocyte-like NP cells. An increasing number of studies demonstrate that notochordal cells (NCs) exert disease-modifying effects, establishing that NC-secreted factors are essential for the maintenance of a healthy intervertebral disc (IVD). However, understanding the role of the NCs is hampered by a restricted reserve of native cells and the lack of robust *ex vivo* cell model. A precise dissection enabled the isolation of NP cells from 4 d post-natal stage mouse spines and their culture into self-organised micromasses. The maintenance of cells' phenotypic characteristics was demonstrated by the presence of intracytoplasmic vacuoles and the immuno-colocalisation of the NC-markers (brachyury; SOX9) after 9 d of culture both in hypoxic and normoxic conditions. A significant increase of the size of the micromass was observed under hypoxia, consistent with a higher level of Ki-67$^+$ immunostained proliferative cells. Furthermore, several proteins of interest for the study of vNCs phenotype (CD44; caveolin-1; aquaporin 2; patched-1) were successfully detected at the plasma membrane of NP-cells cultured in micromasses under hypoxic condition. IHC was performed on mouse IVD sections as control staining. An innovative 3D culture model of vNCs derived from mouse postnatal NP is proposed, allowing future *ex vivo* exploration of their basic biology and of the signalling pathways involved in IVD homeostasis that may be relevant for disc repair.

Keywords: Intervertebral disc, nucleus pulposus cells, vacuolated notochordal cell, *ex vivo* mouse tissue, three-dimensional culture system, hypoxia, tissue engineering.

***Address for correspondence**: Anne Camus, Nantes Université, Oniris, CHU Nantes, INSERM, Regenerative Medicine and Skeleton, RMeS, UMR 1229, F-4400 Nantes, France
Email: anne.camus@univ-nantes.fr

List of Abbreviations

AF	annulus fibrosus
ANOVA	analysis of variance
AQP2	aquaporin 2
BSA	bovine serum albumin
CAV1	caveolin-1
CEP	cartilage endplate
CLC	chondrocyte-like cell
CM	conditioned media
DAB	3, 3 -diaminobenzidine
DIC	Confocal differential interference contrast microscopy
DMEM	Dulbecco's modified Eagle's medium
ECM	extracellular matrix
FCS	foetal calf serum
HBSS	Hanks' balanced salt solution
HEPES	4-(2-hydroxyethyl)-1-piperazineethanesulfonic acid
HES	haematoxylin eosin saffron
HIFs	hypoxia inducible factors
HIF-1α	hypoxia inducible factor 1 alpha
IDD	intervertebral disc degeneration
IF	immunofluorescence
IgG	immunoglobulin G
IHC	immunohistochemistry

IVD	intervertebral disc
KSR	Knockout™ serum replacement
LBP	lower back pain
MM	micromass
NC	notochordal cell
NC	notochordal cell
NCM	notochordal cell-derived matrix
NIH	National Institutes of Health
NP	nucleus pulposus
NPC	nucleus pulposus cells
PBS	phosphate buffer saline
PFA	paraformaldehyde
PTCH1	patched-1
RT	room temperature
SEM	standard error of the mean
SHH	sonic hedgehog
SOX9	SRY-Box transcription factor 9
SRY	Sex-determining region Y
TGF-β	transforming growth factor beta
VB	vertebral body
vNC	vacuolated notochordal cell
WNT	wingless-related integration site
WPI	World Precision Instruments
2D	two-dimensional
3D	three-dimensional

Introduction

The IVD is the fibrous cartilage that lies between two adjacent vertebrae. Each disc is divided into three substructures (Pattappa *et al*., 2012). The proteoglycan-rich and highly hydrated NP, localised in the centre of the IVD, is surrounded by the collagen-rich lamellae of the AF. Both NP and AF are connected to the inferior and superior VB by the CEP, a thin layer of hyaline cartilage. IDD occurrence is often associated with aging and commonly results in chronic LBP. IDD is characterised by an impaired balance control of the disc anabolism and catabolism that leads to ECM degradation, cell loss, disc dehydration and appearance of fibrosis. At least, 80 % of individuals will be affected once in their lifetime by LPB with up to 40 % of LBP associated with IDD, making this pathology a major socio-economic burden throughout the world (Wu *et al*., 2020). To date, no etiopathogenic treatment is available. This is largely due not only to the limited understanding of the molecular effectors underlying IDD but also to the insufficient comprehension of the mechanisms which govern the processes of IVD development, growth, and maturation (Colombier *et al*., 2014; Hickman *et al*., 2022; Mohanty and Dahia, 2019; Séguin *et al*., 2018).

Interestingly, one of the most distinctive changes during IVD maturation and aging is the shift in NP cell phenotype. Indeed, the large vacuolated cells or mature vNCs, a vestige of the embryonic notochord, disappear and are replaced by smaller non-vacuolated NPCs often called CLCs because they share similar morphological aspects with articular chondrocytes (Clouet *et al*., 2009; Minogue *et al*., 2010; Richardson *et al*., 2017; Risbud *et al*., 2015). Cell-fate-tracing experiments in mice demonstrated that embryonic notochord gives rise to both NCs and NPCs (Choi *et al*., 2008; McCann *et al*., 2012). Other studies have established that NCs, NC-CM or NCM play a role in IVD homeostasis by promoting CLC proliferation and also through their anti-apoptotic and anti-angiogenic properties (Bach *et al*., 2015; Bach *et al*., 2016a; Bach *et al*., 2018; de Vries *et al*., 2018). It has been proposed that the decline of mature NCs within the NP is a key event associated with the onset of IDD. Increasing the knowledge of the mechanisms and signalling pathways that drive the transformation of the NCs into NPCs, or control the progressive loss of NCs associated with aging, will surely benefit biomedical research for a better definition of the disease and future development of therapeutic strategies against IDD (Bach *et al*., 2022; Lawson and Harfe, 2017; McCann and Séguin, 2016; Peck *et al*., 2017; Richardson *et al*., 2017; Rodrigues-Pinto *et al*., 2018; Smith *et al*., 2011; Williams *et al*., 2019).

Over the last decade, NP cells have also been considered as a potential cell source for IVD cellular therapy approaches. Although many questions remain concerning cellular or molecular mechanisms of action, numerous *in vivo* animal studies identified WNT, hedgehog and TGF-β signalling pathways as key regulators of IVD homeostasis. For instance, SHH signalling has been shown to play a role in the survival of NCs as well as in disc maturation and its maintenance during post-natal growth and aging (Dahia *et al*., 2009a; Dahia *et al*., 2012; Mohanty *et al*., 2019; Rajesh and Dahia, 2018; Winkler *et al*., 2014). Micro environmental factors such as hypoxia or osmolarity, together with mechanical stimuli have been reported as critical physiological regulators (Bian *et al*., 2017; Hunter *et al*., 2007; Palacio-Mancheno *et al*., 2018; Purmessur *et al*., 2013; Spillekom *et al*., 2014). In particular, HIFs, which are key cellular regulators of the hypoxic response in IVD, are found constitutively active in NP cells (Rajpurohit *et al*., 2002). Targeted deletion of the *HIF-1α* gene in the mouse embryonic notochord resulted in cell death and complete disappearance of the NP cells just after birth. Interestingly, cell fate mapping demonstrated that vNCs were replaced by a fibrocartilaginous tissue, a phenotype similar to the change usually observed during early phases of human IDD (Merceron *et al*., 2014).

The study of NCs' role in IVD homeostasis has so far been hampered by a restricted reserve of native disc cells and the absence of a robust cell model. These limitations have hindered the development of new strategies for NCs-based therapeutic interventions to delay degeneration or mediate regeneration of the damaged disc. In addition to the limited access to human NCs, which disappear before skeletal maturation, inefficient expansion associated with de-differentiation and phenotypic alterations in long-term culture systems also render the study of NCs

physiology difficult (Kluba *et al*., 2005; Mern *et al*., 2014;). A variety of *in vitro* studies based on bovine, canine, porcine and rabbit NP cells culture have so far been performed, providing further insight (Arkesteijn *et al*., 2017; Ashraf *et al*., 2020; Gantenbein *et al*., 2014; Humphreys *et al*., 2018; Potier *et al*., 2014; Rosenzweig *et al*., 2017). Despite the preservation of ECM characteristics observed in these different works, NC or NP cellular markers were not consistently described (Risbud *et al*., 2015). A rapid loss of cell phenotype is generally observed in conventional monolayer expansion (2D culture), whereas 3D systems provide better cell phenotype maintenance. Regardless of species-specific differences, results are not conclusive for the necessary and sufficient *in vitro* conditions that apply to NC culture to maintain NC-associated cell characteristics (Williams *et al*., 2021). In this context, the mouse model is interesting in order to overcome approachability and limited quantity of vNCs. The NP of the newborn mice is populated by large cells of notochordal origin that exhibit abundant cytoplasmic vacuoles. These vacuoles are gradually lost during NP growth and maturation. In ageing mice, cells within the NP become vacuole-free NPCs (Mohanty *et al*., 2019; Tam *et al*., 2018).

In the current study, the setting up of a simple and reproducible 3D culture model of vNCs isolated from mouse immature NP tissue is described. Results demonstrated that explanted NP cells are viable, proliferative, and retained phenotypic features *in vitro*, as indicated by the presence of intracytoplasmic vacuoles. Compared to normoxia, the application of hypoxic conditions to this cellular system recapitulates the physiological environment of the native NP cells during their growth phase at early post-natal stages. Evidence is provided that NP cell explants in 3D culture maintain their NC-like phenotype. IF analysis demonstrates that cells also exhibit several proteins that are essential for their *in vivo* function. Overall, this optimised 3D culture model fully recapitulates native NP cell phenotype therefore offering functional perspectives to study signalling pathways directing vNC cellular responses.

Materials and Methods

Mice

Experiments on mice were conducted according to the French and European regulations on care and protection of laboratory animals (EC Directive 86/609, French Law 2001-486 issued on June 6, 2001). Newborns were obtained 4 d after delivery (4 d post-natal, P4) from spontaneous pregnant mice from the CD1-Swiss background.

Collection of NP cell explants

NP cells were explanted from dissected spines at 4 d post-natal (P4) (see Fig. 1). Surrounding muscles, long bones, and ribs were cut out using scissors (WPI, 14 cm, Sharp/Blunt Straight) in a parallel direction, to isolate the spinal column from the caudal region up to the thoracic region. The caudal region was separated by a cut at the level of the femora. The lumbar region was separated from the thoracic region by a cut below the last rib. The spine segments were then placed in the recovery medium composed by DMEM Glutamax™ (Gibco, 31966-021), 10 % inactivated FCS (PAN technology, P290907, heated at 56 °C for 30 min) supplemented with 1.25 % HEPES (Invitrogen, 15630-056) to preserve tissue viability at RT. The spine segments were further dissected using microsurgery scissors (WPI, 12 cm long, Straight, Sharp/Sharp 15 mm blades) under a dissecting microscope to remove all soft tissues and to expose the anterior and lateral part of the IVDs. Finally, in order to free vertebral bodies and IVDs from other parts of the vertebrae, one blade of the microsurgery scissors was inserted into the spinal canal and the other positioned closer to the VB to cut the bony pedicles on both sides of the vertebrae. The spinal cord (white soft tissue all along the spinal column) and any additional adherent tissues were then removed to expose the posterior part of the IVDs. Once dissected, the spine segments were rinsed in DMEM-HEPES medium without FCS then rinsed in PBS 1× (PBS without Ca, without Mg, Gibco, 20012-019) before the digestion step. To improve isolation efficacy of NP cell explants, enzymatic digestion was performed using a solution of 2.5 % pancreatin (Sigma, P3292) and 0.5 % trypsin (Sigma, T4799) in HBSS 1× (ThermoFisher, 14175053) in a Petri dish on ice for 10 min. This digestion step eases the isolation of NP cells by preventing excessive pressure exerted on the AF and to bypass the difficulty of cutting through the collagen-rich lamellae of the AF. Excessive pressure forces the NP cells out of the AF, resulting in poor recovery in terms of NP cell numbers. To ensure the full viability of the explanted cells and the reproducibility of the MM cultures, a maximum of 6 dissected spine segments were processed through the digestion step simultaneously. The digested spines were then placed back in DMEM-FCS-HEPES recovery medium at 4 °C for at least 5 min before performing the following final steps of the dissection. The digested spine segment was gently held, posterior side orientated down on the dish, using forceps placed at the level of the VB. It was then possible to cut with a scalpel through the AF smoothly, close to the boundary of the CEP, in order to free the whole mass of NP cells and prevent contamination with other tissues. Caution was required at this stage as a cut made too close to the boundary could make NP isolation more difficult. A cut made too far could lead to fragmentation of the NP tissue and dispersion of NP cells, resulting in low yield recovery. The NP cell explants, *i.e.* masses of cells explanted from the NP tissue, were transferred, using a fine tip pipette, in DMEM-FCS-HEPES recovery medium in a small Petri dish on ice. These final steps were repeated for all the IVDs

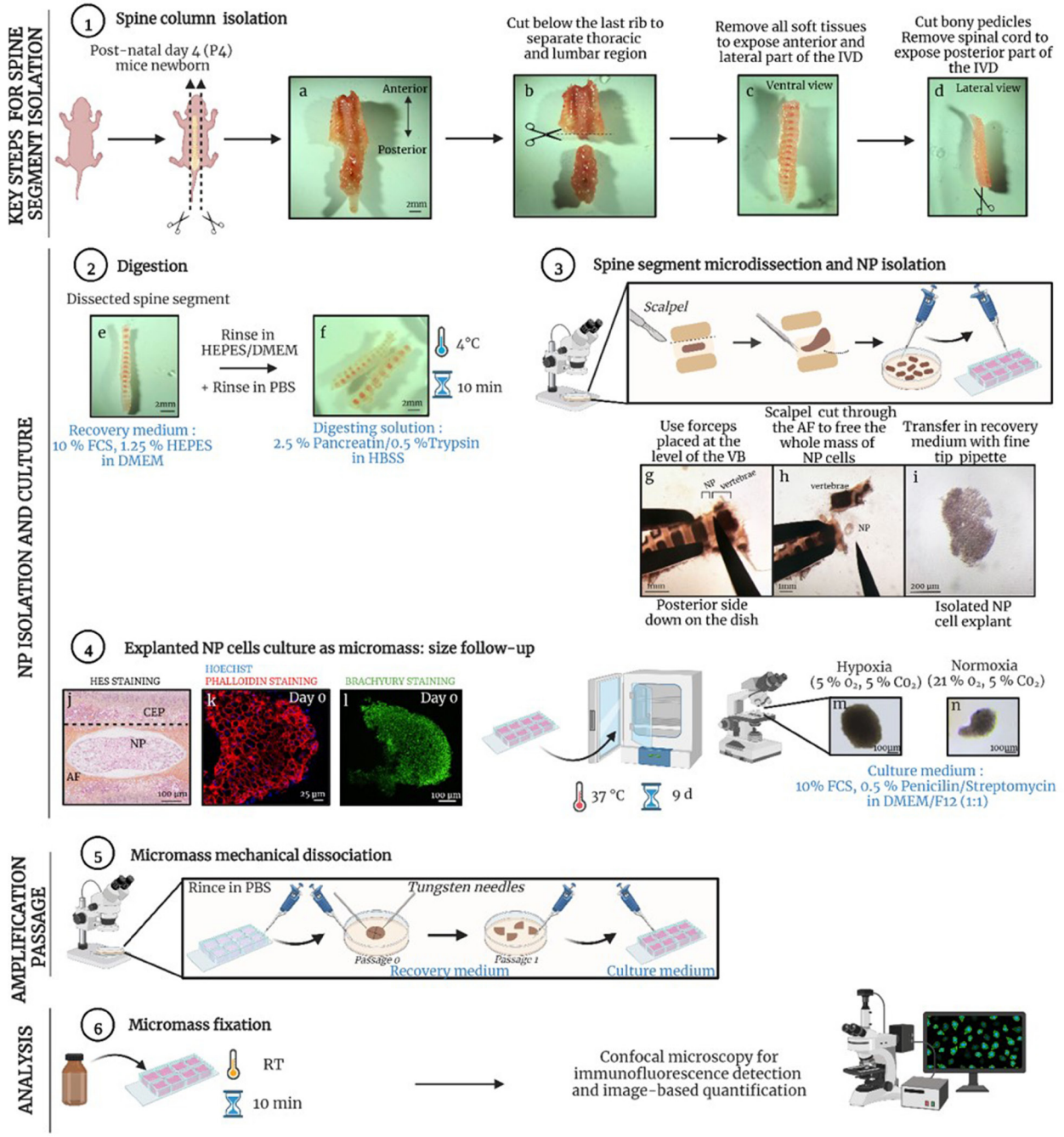

Fig. 1. Schematic representation of the standard operating procedure for the 3D *ex vivo* mouse NP cell explants culture model. NP cells were explanted from dissected spines at 4 d post-natal (P4). (1) Spine column isolation: (**a**,**b**) surrounding muscles, long bones, and ribs were cut out to isolate thoracic and lumbar regions. (**c**,**d**) The spine segments were further dissected to free VBs and IVDs. (2) Digestion: (**e**,**f**) dissected spine segments were incubated in a pancreatin / trypsin digesting solution in HBSS. (3) Spine segment microdissection and NP isolation: (**g**) Forceps were placed at the level the VB. (**h**) A scalpel was used to cut through the AF close to the boundary of the CEP, as indicated by the black dotted line on the IVD section stained with HES in (**j**), enabling the whole mass of NP cells to be collected easily. Freshly explanted mass of NP cells shown in (**i**) was transferred in DMEM-HEPES-FCS recovery medium on ice while microdissection steps were repeated for all IVDs. (4) Explanted NP cells in 3D suspension culture : self-organised MMs' size follow-up under hypoxia or normoxia for 9 d, (**k**) freshly explanted mass of NP cells following microdissection step 3 stained with phalloidin and Hoechst at day 0 (*n* MM = 6) and (**l**) stained for brachyury using IF assay at day 0 (*n* MM = 3). (**m**,**n**) MMs were observed and imaged every day with a light microscope. (5) MM mechanical dissociation: after 9 d of culture in suspension, amplification passage was performed by mechanical dissociation of the explanted NP cell MM with tungsten needles into 4 smaller clumps expanded further in culture for another 9 d. (6) Following culture, MMs were fixed and analysed for specific markers. Created with BioRender.com.

of the digested spine segment. The dissection of 20 spine segments (thoracic and lumbar regions) isolated from 10 new-born mice was necessary to ensure, on average, the generation of 80 MMs after 9 d culture.

Culture of NP cell explants

The explanted masses of NP cells were transferred into culture medium consisting of DMEM Glutamax™/ F12 Nut Mix Glutamax™ (Gibco, 31765-027) (1:1) with 10 % FCS and 0.5 % penicillin / streptomycin (Invitrogen,15140-122) in an uncoated hydrophobic chamber slide (4 NP per well in an 8 well µ-slide, Clinisciences, 80821) to allow their culture into self-organised MMs, in hypoxic (5 % O_2; 5 % CO_2; 37 °C) or normoxic (21 % O_2; 5 % CO_2; 37 °C) environment. These chamber slides were cost-effective for the culture of MMs in suspension in low reagent volumes and were also suitable for immunoreactions. The high optical quality of the coverslip bottom allows high-resolution imaging (DIC and Confocal microscopy). In order to reduce the level of cell death in the explants, it was necessary to equilibrate the medium of culture dishes beforehand in the relevant O_2/CO_2 concentration at 37 °C, for a minimum of 1 h. Note that the culture of NP cells can be performed in a culture medium containing KSR (Fisher Scientific Gibco 15611882), a defined, serum-free, supplement that replaces the FCS (data not shown). KSR is recommended for functional assays that record cellular response to a given stimulation, such as the supplementation of specific growth factors or small inhibitors. Media change was carried out every 2 d

Table 1: Reagents and antibodies used for IHC and IF.

Antigen retrieval				
Buffer	**Reference**	**Dilution**	**Dilution solution**	**Application**
Citrate	Diapath, T0050	1:10	Distilled water	CAV1 IHC 20 min at 90°C
EDTA	Diapath, T0100	1:10	Distilled water	Ki-67, PTCH1 IHC 20 min at 90°C
Proteinase K	Invitrogen, 10005393	1:100	PBS	Brachyury IHC 1h at 37°C
Primary antibodies				
Antibody	**Reference**	**Dilution**	**Dilution solution**	**Application**
Brachyury (T)	R&D, AF2085	1:400	PBS 1× + 1 % BSA	IF
		1:75	DAKO buffer	IHC
SOX9	Abcam, ab5535	1:1000	PBS 1× + 1 % BSA	IF
Phalloidin	Thermofisher Scientific, A12380	1:200	PBS 1× + 1 % BSA	IF
			PBS 1× + 4% BSA + 0.1 % Triton	IF
Ki-67	Sigma, 175R14	1:200	PBS 1× + 1 % BSA	IF
		1:1600	PBS 1× + 4 % BSA + 0.1 % Triton	IHC
Caspase-3	Cell signalling, 9661	1:500	PBS 1× + 4 % BSA + 0.1 % Triton	IF
		1:1600		IHC
CAV1	Clinisciences, GTX-100205	1:100	PBS 1× + 1 % BSA	IF
	BD Sciences, 610407	1:200	DAKO buffer	IHC
PTCH1	Sant Cruz, sc-6149	1:150	PBS 1× + 1 % BSA	IF
		1:75	DAKO buffer	IHC
AQP2	Abcam, 62628	1:500	PBS 1× + 1 % BSA	IF
CD44	Ab41478	1:500	PBS 1× + 1 % BSA	IF
Secondary antibodies				
Alexa Fluor-488	Abcam	1:1200	PBS 1× + 1 % BSA	IF
Alexa Fluor-568	Abcam	1:1200	PBS 1× + 1 % BSA	IF
Anti-mouse IgG	DAKO, E0433	1:500	DAKO buffer	IHC
Anti-rabbit IgG	DAKO, E0432	1:500	PBS 1× + 4 % BSA + 0.1 % Triton	IHC
Anti-goat IgG	Abcam, 208000	1:500	DAKO buffer	IHC
	Santa Cruz sc-2961	1:500		

using an Axio Zoom.V16 (Zeiss) microscope. MMs were observed and imaged every day using a light microscope (Leica microsystems CMS GmbH). Images were analysed using ImageJ software (NIH) using the polygon selection tool to determine manually the outer edge of the MM and quantify the MM surface area.

IF and calcein-AM staining

Freshly explanted masses of NP cells and MMs from explanted NP cells, cultured for 9 d, were fixed for 10 min in 4 % PFA (Electron Microscopy Sciences, 15714) at RT. Cells were permeabilised with 0.5 % Triton X-100 (Sigma, T8787) for 20 min, blocked with 3 % BSA (Sigma, A9647) in PBS for 30 min and incubated overnight at 4 °C with optimum dilution of primary antibodies against brachyury, SOX9, Ki-67, CAV1, AQP2, CD44 or PTCH1 and with Alexa Fluor 568 phalloidin to label actin filaments (Table 1). Samples were then washed and incubated at RT for 1 h with relevant secondary antibodies (Table 1). Nuclei were stained with Hoechst (Invitrogen, H3569) for 20 min and MMs were post-fixed in 1 % PFA for 10 min and stored at 4 °C in Citifluor™ AF1 (Electron Microscopy Sciences, 1179 70-25), a non-hardening antifading / anti-bleaching mounting medium.

Calcein-AM staining was performed to visualise intracytoplasmic vacuoles in explanted NP cells MMs using a LIVE DEAD® viability/cytotoxicity reagents (1:2000; Invitrogen, L3224) for 20 min. MMs were imaged in Z-stacks using a confocal microscope (A1RS, Nikon, Champigny sur Marne, France). Images were analysed using Image J software (NIH). Nuclei counting was performed to determine cell density of the MMs. In addition, T^+/$Ki67^+$ and T^+/$caspase3^+$ immunostained cells' quantifications were performed to evaluate the difference between hypoxia and normoxia culture conditions. To achieve these goals, collections of 5 multiple focal planes (Z-stack imaging) at 10 µm interval were analysed per MM. The surface area of each MM was determined manually using the ImageJ polygon selection tool and the quantification of nuclei or immunopositively stained cells was done manually using the ImageJ multi-point tool.

Immunohistochemistry

Spines from newborn 4 d old mice (P4) were dissected, separated into 3 regions (thoracic, lumbar, and caudal) and fixed in 4 % PFA for 24 h at 4 °C. Spine segments were decalcified (EDTA 0.5 mol/L pH = 7.5, Euromedex, EU0007) for 7 d at 4 °C before paraffin embedding for sectioning (5 µm thick) in the coronal plane. After the antigen retrieval step (as described in Table 1) sections were incubated for 20 min in H_2O_2 3 % (Sigma, H1009) in PBS 1X followed by 30 min in blocking solution. Different blocking solutions were used: 10 % goat serum (Sigma, G9023), 4 % BSA in PBS 1× for anti-CAV1 and Ki-67; 10 % goat serum, 4 % BSA and 0.1 % Triton in PBS 1X for PTCH1 and caspase-3; and 10 % FCS, 4 % BSA in PBS 1× for brachyury. After a washing step, sections were finally incubated overnight at 4 °C with corresponding primary antibodies (Table 1). After three PBS 1× rinses of 5 min, sections were incubated for 1 h in a solution of secondary IgG conjugated with biotin (Table1). Revelation was performed after 45 min incubation in streptavidin-peroxidase solution (Sigma, P0397) and in a solution of DAB substrate (GBI labs, C02-12). Nuclei were stained with Mayer haematoxylin. Stained sections were mounted using Eukitt (Kindler GmbH; B0914) and scanned using a Hamamatsu Nanozoomer HT (Hamamatsu Photonics KK, Hamamatsu City, Japan) digital scanner at 40× magnification.

Statistical analysis

Data of MM size measurement are presented as mean ± SEM. The statistical analyses were performed using Graph Pad Prism 6.0® software (GraphPad, San Diego, California, USA). For MMs surface area measurement, statistical significance was determined for the number of MMs analysed (n) and the number of independent experiments (N) respectively, using two-way ANOVA followed by Bonferroni's multiple comparisons test. Difference in the mean (± SEM) of nuclei or of immunofluorescent positive cells was determined using Mann-Whitney test. Statistical significance was set for p values < 0.05 for all experiments. Data are representative of the number of independent experiments (N) and number of MMs analysed (n) as indicated in the figure legends.

Results

Maintenance of cellular identity in 3D *ex vivo* culture model

Using explanted mouse NP cells at post-natal stage day 4 (P4), which are predominantly composed of vNCs (Fig. 1**i-l**), a 3D suspension culture model was developed to investigate post-natal cell growth and phenotype. This scaffold-free culture model consists of NP cell explants, *i.e.* vNCs that are self-organised into a MM (Fig 1.**m**,**n**). A standard operating procedure, including step-by-step instructions to efficiently achieve the isolation of high quality of NP cell explants and the reproducibility of the MM culture, is described in Materials and Methods and the accompanying Fig. 1.

To study the effect of the microenvironment oxygen concentrations on explanted NP cells' identity and proliferation, MMs cultured under hypoxic (5 % O_2; 5 % CO_2; 37 °C) or normoxic (21 % O_2; 5 % CO_2; 37 °C) conditions were compared. The characteristic and behavioural changes of NP cells were assessed in this 3D culture model system over a 9 d period. First, the cellular architecture was assessed following phalloidin and Hoechst staining performed on IVD histological sections of postnatal mouse spine collected at P4 (control) or on whole-mount MMs (Fig. 2**a-c'**). Numerous cells were detected under

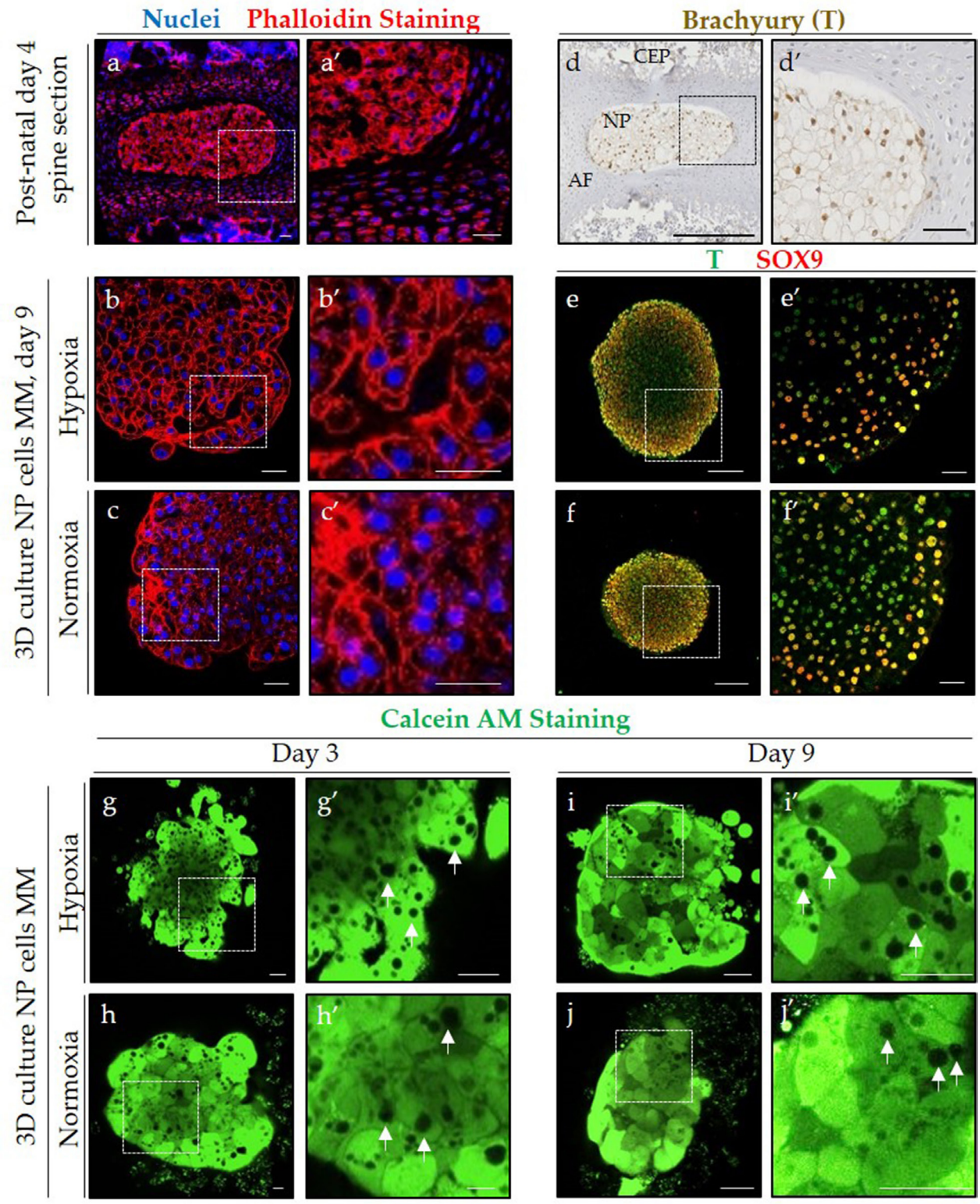

Fig. 2. Maintenance of cellular identity following 9 d culture under hypoxic and normoxic conditions. (**a**,**a′**) Validation of phalloidin staining by in a post-natal P4 mice spine section. Scale bars = 25 μm. (**b**-**c′**) Representative phalloidin fluorescence signal (nuclei are marked in blue by Hoechst) in explanted NP cells (*N* = 3; *n* MM = 3 per condition). Scale bars = 25 μm. (**d**,**d′**). Validation of brachyury (T) antibody by IHC in a post-natal P4 mice spine section. (**d**) Scale bar = 250 μm, (**d′**) scale bar = 50 μm. (**e**-**f′**) Representative IF for T (brachyury) / SOX9 proteins in explanted NP cells cultured under hypoxia (*N* = 15 ; *n* MM = 26) and normoxia (*N* = 9 ; *n* MM = 9), respectively. (**e**,**f**) Scale bar = 100 μm; (**e′**,**f′**) scale bar = 25 μm. (**g**-**h′**) Calcein-AM staining in explanted NP cells cultured for 3 d and (**i**-**j′**) 9 d under hypoxia or normoxia (*N* = 2/day of analysis and *n* MM = 2 per condition). White arrows indicate intracytoplasmic vacuoles. Scale bars = 25 μm.

both hypoxic and normoxic conditions, including in the core of the MMs. Furthermore, confocal imaging of the phalloidin staining revealed a densified meshwork of actin filaments, characteristic of vNCs (Hunter *et al*., 2004). No obvious structural changes could be observed when these MMs were compared to freshly explanted mass of NP cells stained with phalloidin and Hoechst immediately following microdissection (day 0; Fig. 1**k**). Next, whether the vNCs' identity was maintained in the 3D culture model was investigated. From early organogenesis, the transcription factor brachyury (T) is expressed exclusively in the notochordal lineage and further maintained following birth in NCs constituting the NP in both mice and humans (Peck *et al*., 2017; Rodrigues-Pinto *et al*., 2016). Brachyury was detected in all cells of the NP at P4, as shown by IHC control staining on mouse spine histological sections (Fig. 2**d**,**d'**). SOX9 transcription factor is detected both in NCs and somite-derived sclerotomal cells (Lefebvre, 2019). In order to discriminate between these two cell-types and adequately assess the phenotype of NP cells, T and SOX9 co-immunostaining analysis was performed on fixed and permeabilised MMs following 9 d of culture. MMs showed colocalisation of T and SOX9 fluorescent signals after 9 d of culture under both conditions (Fig. 2**e-f'**). The co-detection of these two transcription factors demonstrated the maintenance of NP cell phenotype under both hypoxic and normoxic conditions. The presence of cytoplasmic vacuoles in the explanted NP cells was explored further. This is a phenotype that has been identified as one cellular aspect conserved from IVD embryonic formation to juvenile NP growth and maturation (Wang *et al*., 2017). Intracellular vacuoles can be visualised following a calcein-AM staining, which results in an even distribution of fluorophore throughout the cytoplasm, but with complete exclusion of fluorophore from the vacuole lumen (Hunter *et al*., 2007). The presence of intracytoplasmic vacuoles was confirmed at 3 and 9 d of culture under both conditions (Fig. 2**g-j'**). Taken together, these results validated the maintenance of cellular identity over the culture period in this 3D *ex vivo* model of explanted NP cells.

Table 2. Values (min; max) of MM size area in μm² following culture

Conditions	2-3 d	4-5 d	6-7 d	8-9 d
MM				
Hypoxia	25 497; 388 615	25 704; 395 648	27 757; 456 045	32 033; 456 045
Normoxia	44 425; 235 914	25 451; 244 161	25 337; 203 924	15 320; 261 447
MM after 1 passage				
Hypoxia	16 430; 105 267	25 696; 121 995	34 506; 170 087	48 191; 280 438

Hypoxic environment promotes explanted NP cells proliferation

To determine the suitable culture condition for the amplification of explanted NP cells, growth of the MMs in culture was quantified by measuring the MM surface area day after day. Time-course analysis showed a statistically significant increase in MM size after 9 d in culture under hypoxia. In contrast, no difference in MM size was found when cultured under normoxia (Fig. 3**a**,**b**). Image-based quantifications suggested a tendency for a higher cell density in MMs cultured under hypoxia compared to normoxia at day 9, although not statistically significant (Fig. 3**c**). A previous study has shown that NP cell proliferation terminates at P21, while the onset of apoptotic events begin at 1 month old (Dahia *et al*., 2009b). To analyse the proliferation status, the nuclear

Fig. 3. (On next page) **Hypoxic environment promotes explanted NP cell growth and proliferative capacities.** (**a**) Light microscopy images of MM in culture under hypoxia or normoxia over 9 d of culture, D = days. Scale bars = 100 μm. (**b**) MM growth is represented as the evolution of the MM surface area in μm², based on the value of the outer edge of the MM. (**c**) Image-based quantification of the mean number of nuclei in a MM cultured under hypoxia or normoxia at 9 d. *N*: number of experiment. The number of analysed NP MMs was over 130/d and per condition. Mean ± SEM. ** $p < 0.01$. (**d**,**d'**) Validation of the proliferation-related Ki-67 antibody by IHC in post-natal P4 mouse spine section. Black arrowhead: Ki-67 positive cells in NP contour. (**d**) Scale bar = 250 μm; (**d'**) scale bar = 50 μm. (**e-f'**) Representative IF for T / Ki-67 proteins in explanted NP cells cultured under hypoxia (*N* = 13; *n* MM = 27) and normoxia (*N* = 9; *n* MM = 10) for 9 d. (**e**,**f**) Scale bars = 100 μm; (**e'**,**f'**) scale bars = 25 μm. (**g**) Image-based quantification of the mean number of T^+/Ki-67$^+$ cells in MM in culture under hypoxia (*N* = 12; *n* MM = 25) or normoxia (*N* = 8; *n* MM = 9) at 9 d. Mean ± SEM; **** $p < 0.0001$. On average, 50 T+/Ki-67$^+$ cells/MM were observed under hypoxia for every 5 T^+/Ki-67$^+$ cells/MM under normoxia conditions. (**h**,**h'**) Validation of the apoptosis-related antibody caspase-3 by IHC in post-natal P4 mouse spine section. Black arrowhead: caspase-3 positive cells in the VB. (**h**) Scale bar = 250 μm; (**h'**) scale bar = 50 μm. (**i-j'**) Representative IF for T/caspase-3 proteins in explanted NP cells cultured under hypoxia (*N* = 4; *n* MM = 8) or normoxia (*N* = 4; *n* MM = 6) for 9 d. (**i**,**j**) Scale bars = 100 μm; (**i'**,**j'**) scale bars = 25 μm. (**k**) Image-based quantification of the mean number of T^+/caspase-3$^+$ cells in MM under hypoxia (*N* = 3; *n* MM = 8) or normoxia (*N* = 3; *n* MM = 4) for 9 d. Mean ± SEM; Mann-Whitney test; ns: non-significant. On average <1 T^+/caspase-3$^+$ cell/MM was observed under both hypoxia and normoxia.

marker Ki-67 was chosen, which is highly expressed in proliferating cells (G1, S, G2 and M phases of the cell cycle) but undetectable in G0-phase cells. Specific distribution of Ki-67$^+$ immunostained cells was observed within the NP and the CEP at P4 on control spine histological sections (Fig. 3**d**,**d'**). Interestingly, Ki-67$^+$ cells were consistently found at the periphery of the NP. In line with the differences observed for the MM growth at day 9, immunodetection assay showed a high level of the Ki-67$^+$ proliferative cells in MMs cultured under hypoxia compared to normoxia (Fig. 3**e**-**f'**). Indeed image-based quantifications revealed a marked increase of the mean value of T$^+$/Ki-67$^+$ cells in MMs cultured under hypoxia compared to normoxia (Fig. 3**g**). From these analyses, it was concluded that a hypoxic environment promoted

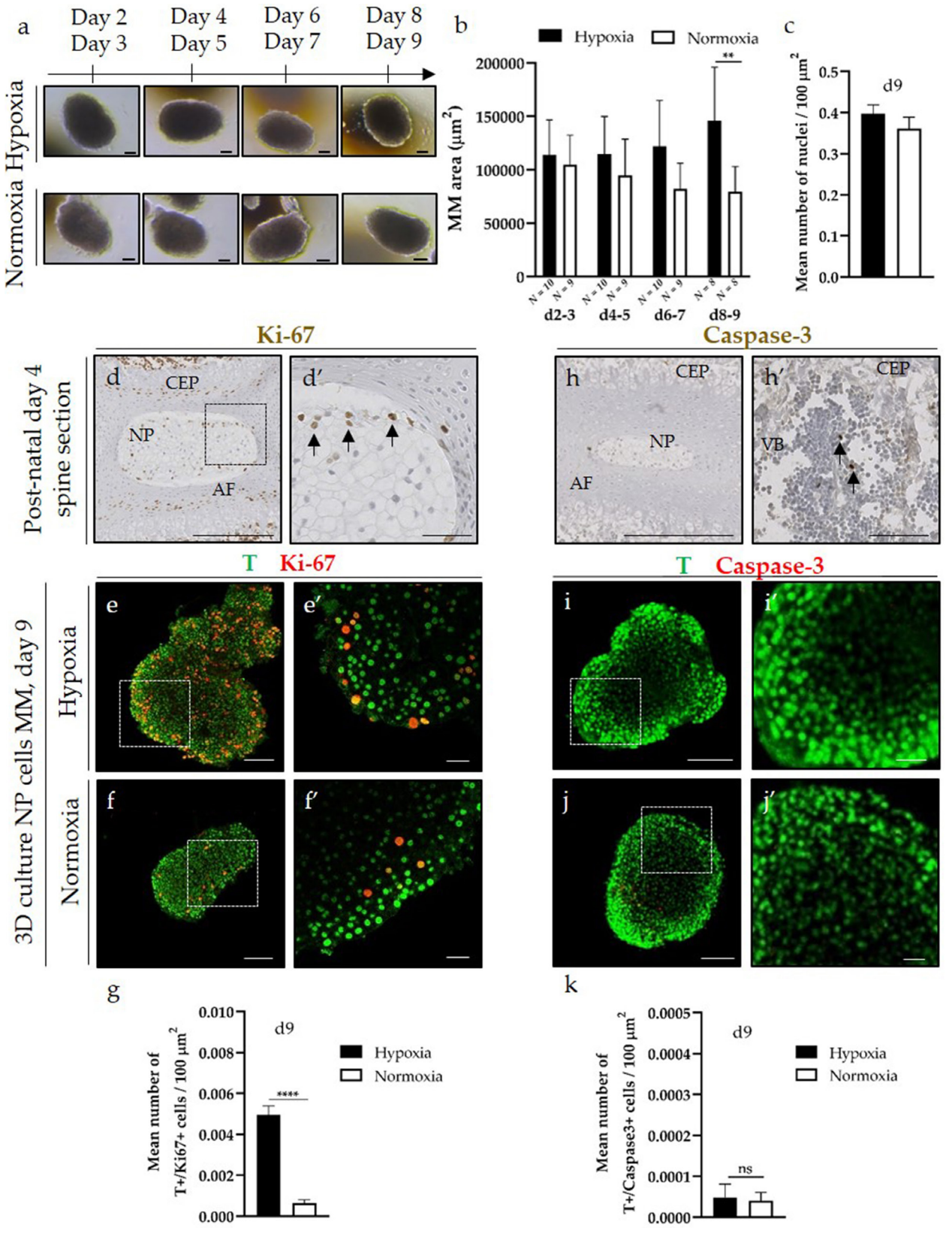

proliferation of explanted NP cells and MM growth. Finally, in order to analyse apoptotic events in the NP, the caspase-3 marker was used, which was only found in rare cells at P4 in the VB region on control spine histological sections (Fig. 3**h**,**h'**). The number of detected apoptotic cells was negligible in all analysed conditions (Fig. 3**i**-**j'**). Image-based quantifications revealed similarly low values of T^+/caspase-3^+ cells in MMs cultured under hypoxia or normoxia (Fig. 3**k**). These results indicated no significant effect on cell viability over the culture period in this 3D *in vitro* model of explanted NP cells.

Optimised tool to explore vNCs biology and cellular behaviour

To validate the functionality of this 3D model system and its usefulness for the study of signalling pathways involved in cellular responses, the presence of several proteins of interest following 9 d of culture under hypoxia was analysed. IF assay was used to assess, in explanted NP cell MMs, the distribution of the protein CD44, which has been shown to be expressed during IVD embryonic development and post-natal growth and co-detected with hyaluronic acid in rat NP (Stevens *et al*., 2000). CAV1 protein was also analysed, a major component of caveolae – specialised membrane microdomains of the plasma membrane (Parton *et al*., 2020). Furthermore, the presence of aquaporin proteins was investigated, which are key players in water/ion transport at the plasma membrane and have been shown to be expressed in both canine and human healthy IVDs (Snuggs *et al*., 2019). Finally, from the perspective of studying the SHH signalling pathway, which has been shown to be essential for IVD embryonic development as well as post-natal growth, PTCH1 protein immunodetection was performed. IHC staining performed at P4 on control mouse spine histological sections showed

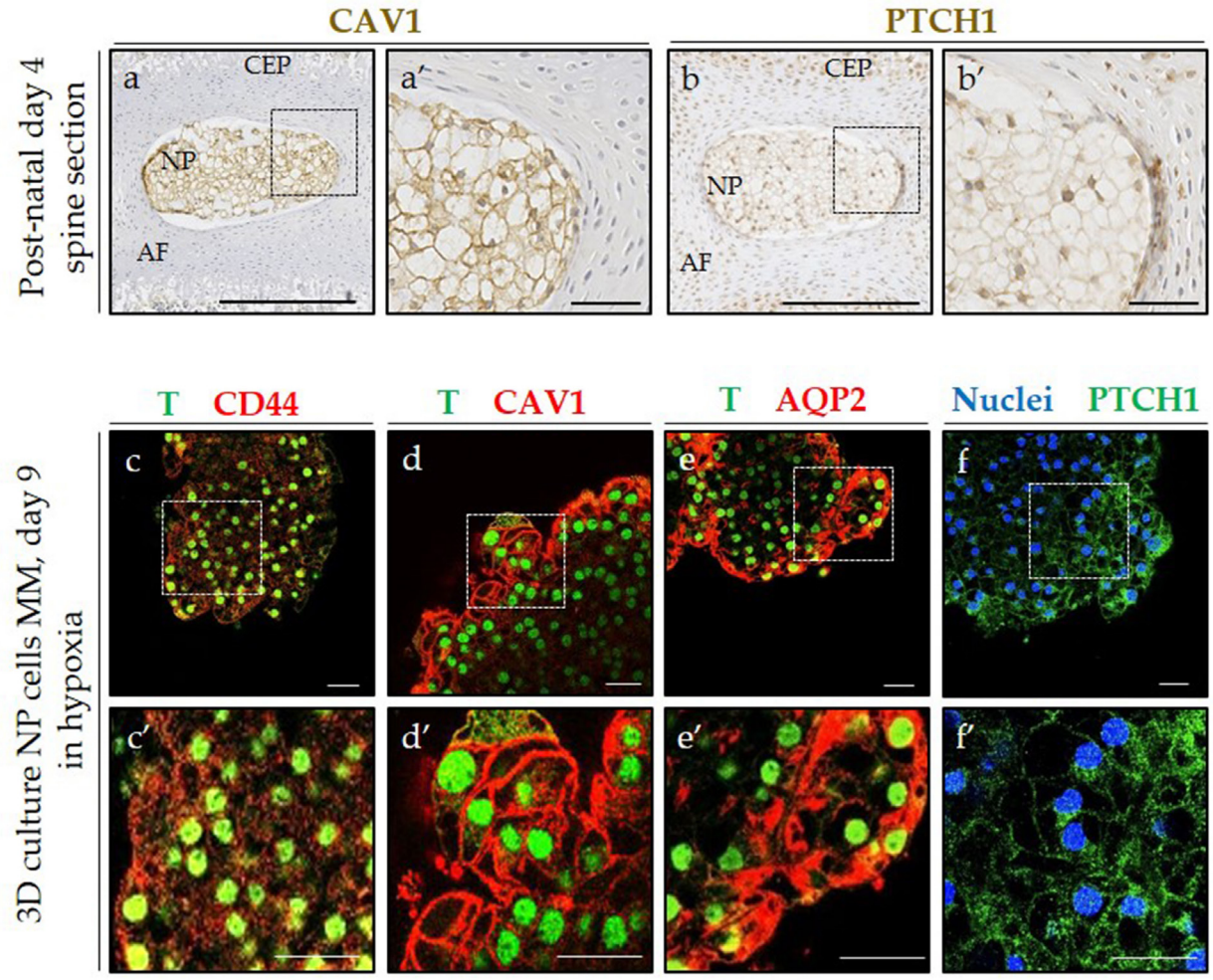

Fig. 4. The 3D culture model of vNCs permit the functional analysis of signalling pathways involved in cellular response during IVD growth. (**a**,**a'**) Validation of CAV1 and (**b**,**b'**) PTCH1 antibodies by IHC in post-natal P4 mouse spine section. (**a**,**b**) Scale bars = 250 μm; (**a'**,**b'**) scale bars = 50 μm. (**c**,**c'**) Representative IF for T/CD44 proteins (N = 2; n MM = 4), (**d**,**d'**) T/CAV1 proteins (N = 12; n MM = 22), (**e**,**e'**) T/AQP2 (N = 2; n MM = 2) and (**f**,**f'**) PTCH1 (N = 3; n MM = 4) in explanted NP cells cultured under hypoxia. Nuclei were stained in blue with Hoechst. CD44 is the hyaluronic acid receptor (component of NP ECM), CAV1 is a caveolar component implicated in IVD degeneration process, AQP2 is implicated is NP osmotic modulation and PTCH1 is a Hedgehog signalling pathway receptor. (**c**-**f'**) Scale bars = 25 μm.

that CAV1 protein localised, as expected, at the plasma membrane – specifically in the NP (Fig. 4**a**,**a'**). The PTCH1 receptor was distributed at the membrane as well as in perinuclear cell area of the NP (Fig. 4**b**,**b'**). Consistently, IF analysis of the MMs after 9 d of culture under hypoxia showed that CD44, CAV1, and AQP2 signals were localised at the plasma membrane of explanted NP cells (Fig. 4**c**-**e'**). Similar to IHC staining performed at P4 on control histological sections, the PTCH1 receptor IF signal was observed at the plasma membrane and also in the perinuclear region in explanted NP cell MMs (Fig. 4**f**,**f'**). Interestingly, explanted NP cells can be expanded after 9 d in culture following mechanical dissociation of the MM into smaller clumps (Fig. 1, step 5). Clumps of NP cells will grow further in culture for another 9 d as shown by time course analysis of MM size (Fig. 5**a**,**b**). Following one passage and further amplification in culture, MMs showed a tendency to reduce in size after 9 d; however, the identity of NP cells (co-detection of T and SOX9 markers), proliferation (detection of Ki-67 marker) and cellular behaviour (co-detection of T and CAV1 markers) were maintained for a longer time, up to day 14 (Fig. 5**c**-**f'**).

Discussion

This work aimed at developing a simple and reproducible 3D *in vitro* culture model to study basic biology and function of vNCs isolated from new-born mice. Advantage was taken of the use murine immature NP tissue, which is populated by large cells of notochordal-origin that exhibit abundant cytoplasmic vacuoles. Here is described, step by step, the setting up of the 3D culture system and the optimised conditions that maintains cell viability

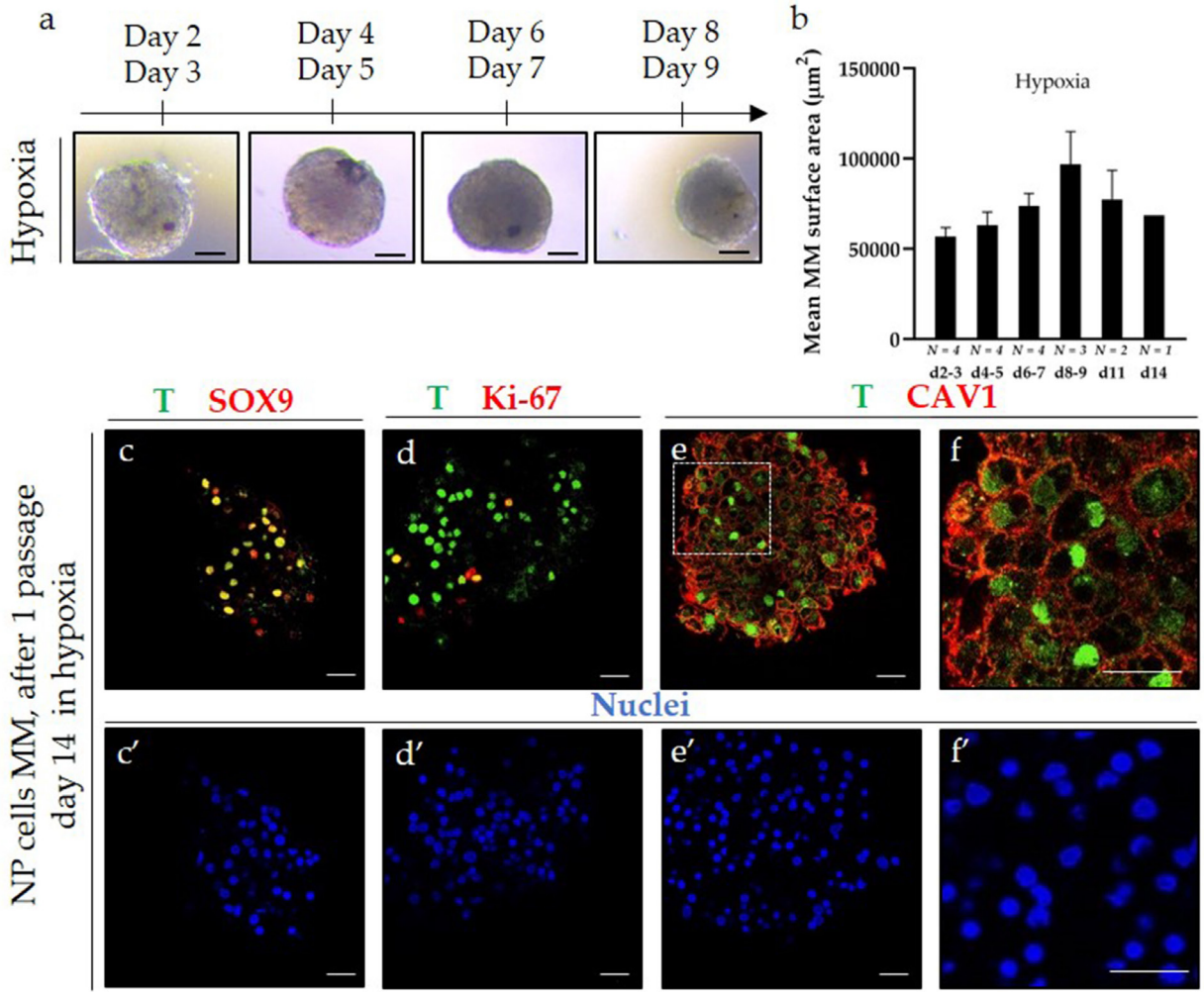

Fig. 5. Assessment of growth, cell identity, proliferation, and cell behaviour of explanted NP cells following one passage (amplification) and cultured under hypoxia. (**a**) Light microscopy images of MM over 9 d of culture. Scale bar = 100 µm. (**b**) MM growth is represented as the evolution of the MM surface area in µm², based on the value of the outer edge of the MM. *N*: number of experiment; number of MM ≥ 60/d. Mean ± SEM. (**c**-**f**) Representative IF for T (brachyury)-SOX9 proteins (*N* = 1; *n* MM = 1), T-Ki67 proteins (*N* = 1, *n* MM = 1) and T-CAV1 proteins (*N* = 1, *n* MM = 1) in NP-explanted cells after 1 passage cultured under hypoxia for 14 d. (**c'**-**f'**) Nuclei staining. (**c**-**f'**) Scale bars = 25 µm.

and enables MM growth in suspension. The results demonstrated that the proposed 3D model system successfully amplified vNCs while preserving their phenotype *i.e.* the intracytoplasmic vacuoles and the NC characteristic markers brachyury and SOX9, over 9 d of culture. Of note, explanted NP cells retained their characteristic features *in vitro*, without going through a phase of dedifferentiation generally reported when cells are expanded in 2D culture. Existing 3D cell models and technologies have largely demonstrated that they overcome the deficiencies of 2D culture, uplifting cell culture to a more physiologically relevant dimension (Nguyen *et al*., 2022; Shamir and Ewald, 2014). Evidence is also provided that the size of the MMs increased significantly under hypoxic compared to normoxic conditions. Moreover, more Ki-67^{+} immunostained proliferative cells were observed in culture under hypoxia. Hypoxia was therefore chosen for the development of the culture system, as it appears to better mimic the physiological environment of native NP cells during their growth phase at early post-natal stages.

The development of a relevant 3D cell model systems is required for the improved understanding of the basic biology of vacuolated cells, their maturation and proliferation. Thus, the currently reported *ex vivo* 3D model will allow detailed investigations of vNCs cellular behaviour and signalling response to biological effects, mimicking *in vivo* environments such as age or degeneration. In this study, the feasibility of using the proposed 3D model to examine either environmental changes influencing cell-matrix interactions or cell signalling, or study changes mediated through mechanical and osmolar stimuli, was also assessed. Evidence is also provided for the presence of CD44, CAV1, AQP2 and PTCH1 proteins at the plasma membrane of the explanted NP cells in MMs. This 3D system is optimised for the detection of proteins of interest involved in NP post-natal growth or IVD degeneration and should be a useful tool to go further in the study of signalling pathways involved in IVD homeostasis. CD44, a type I transmembrane glycoprotein, has been proposed as a receptor for the anchorage of hyaluronic acid in the pericellular matrix of rat NP cells. A decrease of CD44 expression in the NP has been associated with increased age (Stevens *et al*., 2000). CAV1 have been identified as key proteins in the cellular response to mechanical stress in numerous cell types (Boyd *et al*., 2003; Sedding *et al*., 2005; Sinha *et al*., 2011). Remarkably, the absence of caveolae in *Cav1-null* mice resulted in premature disc degeneration as early as 1.5 months of age (Bach *et al*., 2016b; Smolders *et al*., 2013). Interestingly, CAV1 protein has been reported in both healthy and degenerated NP cells of different species although the precise implication of the caveolae for IVD homeostasis has not yet been fully elucidated. Several members of the aquaporin family of transmembrane channel proteins are involved in the cellular response to osmotic change that occurs naturally in healthy canine and human NP tissue (Gajghate *et al*., 2009; Johnson *et al*., 2014; Richardson *et al*., 2008; Sadowska *et al*., 2018). AQP2 has been shown to increase with degeneration in human NP (Snuggs *et al*., 2019; Snuggs *et al*., 2021). Recent work using whole mouse IVD organ culture model indicated a role for aquaporin in osmoregulation and, in NC, to NP cell transition during IVD maturation (Palacio-Mancheno *et al*., 2018). The PTCH1 receptor is a direct transcriptional target and negative regulator of the SHH signalling pathway. The SHH pathway is critical for NC maintenance and NP formation during embryonic disc development (Chiang *et al*., 1996; Choi and Harfe, 2011). Even though SHH levels decrease significantly following disc development, the importance of this pathway for many aspects of disc cell growth and differentiation at early postnatal stages has been highlighted (Dahia *et al*., 2012; Peck *et al*., 2017). Further research work is warranted to delineate the exact role of the HH pathway in disc maturation and ageing and its interplay with other signalling pathways in the IVD degeneration process (Bach *et al*., 2019; Kondo *et al*., 2011; Winkler *et al*., 2014). This 3D culture model represents a relevant tool for the modulation of signalling pathways, using drugs, to better characterise cellular response of vNCs and elucidate their mechanisms of action.

Despite its relevance, this model presents limits inherent to the specificity of mouse NP tissue. Vacuolated NCs were isolated from the NP of new-born mice, thus the explanted material is restricted in terms of cell numbers due the small size of the animal. On average, 8 MM could be generated from the dissection of one spine. However, this 3D culture system allowed a relatively good amplification of the vNCs over a 9-day culture period and their passaging, after manual dissociation of the MMs, was possible for further amplification. Therefore, this *ex vivo* system represents a good alternative for the reduction of functional tests performed, usually directly on animals. Based on cell morphology and, in particular, on observations made on phalloidin-stained MMs (at the time of isolation at day 0 and following a period of 9 d culture), it was concluded that the proposed method offers a very good capacity for the isolation of NP cell explants from the IVD, free of AF, CEP or marrow tissue contamination. However, as no AF, CEP or marrow tissue specific markers were tested in this study, it is not possible to formally exclude very-low level contamination of NP cell explants. This model should permit detailed investigations of cellular behaviour and signal transduction events in cells in response to age or a degenerative environment, as well as in response to regenerative treatment. Another limitation to the data interpretation relates to the differences existing in IVD formation and maturation between mice and humans, since mature NCs persist after skeletal maturity in rodents, which is not the case in the human IVD. Consequently, knowledge resulting from studies using this *in vitro* model of NC-like

cells will have to be interpreted with caution and extrapolation to the human situation should only be conducted with support from further translational studies (Gantenbein *et al*., 2015). Nevertheless, the process of ageing of the mouse IVD is well described. Moreover, many studies report the generation of NC- or NP-conditional knockouts for the study of IVD homeostasis, progressing the research on the human disease. In this context, the current model is worthy of interest for studies at the cellular and molecular levels of the phenotypic changes in mature NCs isolated from genetically engineered mice (Tang *et al*., 2022).

In conclusion, a novel and optimised 3D culture model of vNCs has been established that outperforms available 2D culture options. Disappearance of early vNCs, which restrains discal tissue self-renewal and self-repair, is at the origin of the necessity to develop innovative cellular therapy strategies (Binch *et al*., 2021). This is also restricting the study of vNCs function and proliferative capacity. From this point of view, this model will constitute a useful tool to explore fundamental mechanisms and generate new insights on vNCs biology. This 3D model will definitely contribute to the imperative need to better characterise the precise phenotype of cells with the therapeutic potential to regulate disc homeostasis, and to develop innovative clinical approaches counteracting IDD.

Acknowledgments

This research was funded by INSERM and by grants from the Region Pays de la Loire (BIODIV and RFI BIOREGATE-CAVEODISC), Arthritis Foundation (NOTOCH) and the French Society of Rheumatology (SPHERODISC). The authors would like to thank K. Dedieu, A. Henry and C. Chédeville for technical advice. We acknowledge the IBISA MicroPICell facility (Biogenouest), member of the national infrastructure France-Bioimaging supported by the French national research agency (ANR-10-INBS-04) and SC3M facility from SFR Francois Bonamy, University of Nantes. We thank UTE-IRS-UN Animal facilities staff for animal care, breeding, and for their investment in the project. The authors declare no conflict of interest. The funders had no role in the design of the study, analyses, or interpretation of data; in the writing of the manuscript, or in the decision to publish the results.

References

Arkesteijn ITM, Potier E, Ito K (2017) The regenerative potential of notochordal cells in a nucleus pulposus explant. Global Spine **7**: 14-20. DOI: 10.1055/s-0036-1583174.

Ashraf S, Chatoor K, Chong J, Pilliar R, Santerre P, Kandel R (2020) Transforming growth factor β enhances tissue formation by passaged nucleus pulposus cells *in vitro*. J Orthop Res **38**: 438-449. DOI: 10.1002/jor.24476.

Bach FC, de Vries SAH, Krouwels A, Creemers LB, Ito K, Meij BP, Tryfonidou MA (2015) The species-specific regenerative effects of notochordal cell-conditioned medium on chondrocyte-like cells derived from degenerated human intervertebral discs. Eur Cell Mater **30**: 132-146. DOI: 10.22203/ecm.v030a10.

Bach FC, de Vries SAH, Riemers FM, Boere J, van Heel FWM, van Doeselaar M, Goerdayal SS, Nikkels PGJ, Benz K, Creemers LB, Maarten Altelaar AF, Meij BP, Ito K, Tryfonidou MA (2016a) Soluble and pelletable factors in porcine, canine and human notochordal cell-conditioned medium: implications for IVD regeneration. Eur Cell Mater **32**: 163-180. DOI: 10.22203/ecm.v032a11.

Bach FC, Zhang Y, Miranda-Bedate A, Verdonschot LC, Bergknut N, Creemers LB, Ito K, Sakai D, Chan D, Meij BP, Tryfonidou MA (2016b) Increased caveolin-1 in intervertebral disc degeneration facilitates repair. Arthritis Res Ther **18**: 59. DOI: 10.1186/s13075-016-0960-y.

Bach FC, Tellegen AR, Beukers M, Miranda-Bedate A, Teunissen M, De Jong WAM, De Vries SAH, Creemers LB, Benz K, Meij BP, Ito K, Tryfonidou MA (2018) Biologic canine and human intervertebral disc repair by notochordal cell-derived matrix: from bench towards bedside. Oncotarget **9**: 26507-26526. DOI: 10.18632/oncotarget.25476.

Bach FC, Rooij KM, Riemers FM, Snuggs JW, Jong WAM, Zhang Y, Creemers LB, Chan D, Le Maitre C, Tryfonidou MA (2019) Hedgehog proteins and parathyroid hormone-related protein are involved in intervertebral disc maturation, degeneration, and calcification. JOR Spine **2**: e1071. DOI: 10.1002/jsp2.1071.

Bach FC, Poramba-Liyanage DW, Riemers FM, Guicheux J, Camus A, Iatridis JC, Chan D, Ito K, Le Maitre CL, Tryfonidou MA (2022) Notochordal cell-based treatment strategies and their potential in intervertebral disc regeneration. Front Cell Dev Biol **9**: 780749. DOI:10.3389/fcell.2021.780749.

Bian Q, Ma L, Jain A, Crane JL, Kebaish K, Wan M, Zhang Z, Edward Guo X, Sponseller PD, Séguin CA, Riley LH, Wang Y, Cao X (2017) Mechanosignaling activation of TGFβ maintains intervertebral disc homeostasis. Bone Res **5**: 17008. DOI: 10.1038/boneres.2017.8.

Binch ALA, Fitzgerald JC, Growney EA, Barry F (2021) Cell-based strategies for IVD repair: clinical progress and translational obstacles. Nat Rev Rheumatol **17**: 158-175. DOI: 10.1038/s41584-020-00568-w.

Boyd NL, Park H, Yi H, Chool Boo Y, Sorescu GP, Sykes M, Jo H (2003) Chronic shear induces caveolae formation and alters ERK and Akt responses in endothelial cells. Am J Physiol Heart Circ Physiol **285**: H1113-1122. DOI: 10.1152/ajpheart.00302.2003.

Chiang C, Litingtung Y, Lee E, Young KE, Corden JL, Westphal H, Beachy PA (1996) Cyclopia and defective axial patterning in mice lacking sonic hedgehog gene function. Nature **383**: 407-413. DOI: 10.1038/383407a0.

Choi KS, Cohn MJ, Harfe BD (2008) Identification of nucleus pulposus precursor cells and notochordal remnants in the mouse: implications for disk degeneration and chordoma formation. Dev Dyn **237**: 3953-3958.DOI: 10.1002/dvdy.21805.

Choi KS, Harfe BD (2011) Hedgehog signaling is required for formation of the notochord sheath and patterning of nuclei pulposi within the intervertebral discs. Proc Natl Acad Sci U S A **108**: 9484-9489. DOI: 10.1073/pnas.1007566108.

Clouet J, Grimandi G, Pot-Vaucel M, Masson M, Fellah HB, Guigand L, Cherel Y, Bord E, Rannou F, Weiss P, Guicheux J, Vinatier C (2009) Identification of phenotypic discriminating markers for intervertebral disc cells and articular chondrocytes. Rheumatology (Oxford) **48**: 1447-1450. DOI: 10.1093/rheumatology/kep262.

Colombier P, Camus A, Lescaudron L, Clouet J, Guicheux J (2014) Intervertebral disc regeneration: a great challenge for tissue engineers. Trends Biotechnol **32**: 433-435. DOI: 10.1016/j.tibtech.2014.05.006.

Dahia CL, Mahoney EJ, Durrani AA, Wylie C (2009a) Intercellular signaling pathways active during intervertebral disc growth, differentiation, and aging. Spine (Phila Pa 76) **34**: 456-462. DOI: 10.1097/BRS.0b013e3181913e98.

Dahia CL, Mahoney EJ, Durrani AA, Wylie C (2009b) Postnatal growth, differentiation, and aging of the mouse intervertebral disc. Spine (Phila Pa 1976) **34**: 447-455. DOI: 10.1097/BRS.0b013e3181990c64.

Dahia CL, Mahoney E, Wylie C (2012) Shh signaling from the nucleus pulposus is required for the postnatal growth and differentiation of the mouse intervertebral disc. PLoS One **7**: e35944. DOI:10.1371/journal.pone.0035944.

Gajghate S, Hiyama A, Shah M, Sakai D, Anderson DG, Shapiro IM, Risbud MV (2009) Osmolarity and intracellular calcium regulate aquaporin2 expression through TonEBP in nucleus pulposus cells of the intervertebral disc. J Bone Miner Res **24**: 992-1001. DOI: 10.1359/jbmr.090103.

Gantenbein B, Calandriello E, Wuertz-Kozak K, Benneker LM, Keel MJB, Chan SCW (2014) Activation of intervertebral disc cells by co-culture with notochordal cells, conditioned medium and hypoxia. BMC Musculoskelet Disord **15**: 422. DOI: 10.1186/1471-2474-15-422.

Gantenbein B, Illien-Jünger S, Chan SC, Walser J, Haglund L, Ferguson SJ, Iatridis JC, Grad S (2015) Organ culture bioreactors-platforms to study human intervertebral disc degeneration and regenerative therapy. Curr Stem Cell Res Ther **10**: 339-352. DOI: 10.2174/1574888x10666150312102948.

Hickman TT, Rathan-Kumar S, Peck SH (2022) Development, pathogenesis, and regeneration of the intervertebral disc: current and future insights spanning traditional to omics methods. Front Cell Dev Biol **10**: 841831. DOI:10.3389/fcell.2022.841831.

Humphreys MD, Ward L, Richardson SM, Hoyland JA (2018) An optimized culture system for notochordal cell expansion with retention of phenotype. JOR Spine **1**: e028. DOI:10.1002/jsp2.1028.

Hunter CJ, Bianchi S, Cheng P, Muldrew K (2007) Osmoregulatory function of large vacuoles found in notochordal cells of the intervertebral disc running title: an osmoregulatory vacuole. Mol Cell Biomech **4**: 227-237. DOI:*10.3970/mcb.2007.004.227*.

Hunter CJ, Matyas JR, Duncan NA (2004) Cytomorphology of notochordal and chondrocytic cells from the nucleus pulposus: a species comparison. J Anat **205**: 357-362. DOI: 10.1111/j.0021-8782.2004.00352.x.

Johnson ZI, Shapiro IM, Risbud MV (2014) Extracellular osmolarity regulates matrix homeostasis in the intervertebral disc and articular cartilage: evolving role of TonEBP. Matrix Biol **40**: 10-16. DOI: 10.1016/j.matbio.2014.08.014.

Kluba T, Niemeyer T, Gaissmaier C, Gründer T (2005) Human anulus fibrosis and nucleus pulposus cells of the intervertebral disc: effect of degeneration and culture system on cell phenotype. Spine (Phila Pa 1976) **30**: 2743-2748. DOI: 10.1097/01.brs.0000192204.89160.6d.

Kondo N, Yuasa T, Shimono K, Tung W, Okabe T, Yasuhara R, Pacifici M, Zhang Y, Iwamoto M, Enomoto-Iwamoto M (2011) Intervertebral disc development is regulated by wnt/β-catenin signaling. Spine (Phila Pa 1976) **36**: E513-518. DOI:10.1097/BRS.0b013e3181f52cb5.

Lawson LY, Harfe BD (2017) Developmental mechanisms of intervertebral disc and vertebral column formation. Wiley Interdiscip Rev Dev Biol **6**. DOI:10.1002/wdev.283.

Lefebvre V (2019) Roles and regulation of SOX transcription factors in skeletogenesis. Curr Top Dev Biol **133**: 171-193. DOI: 10.1016/bs.ctdb.2019.01.007.

McCann MR, Tamplin OJ, Rossant J, Seǵuin CA (2012) Tracing notochord-derived cells using a Noto-cre mouse: implications for intervertebral disc development. Dis Model Mech **5**: 73-82. DOI: 10.1242/dmm.008128.

McCann M, Séguin C (2016) Notochord cells in intervertebral disc development and degeneration. J Dev Biol **4**: 3. DOI:10.3390/jdb4010003.

Merceron C, Mangiavini L, Robling A, Wilson TL, Giaccia AJ, Shapiro IM, Schipani E, Risbud MV (2014) Loss of HIF-1α in the notochord results in cell death and complete disappearance of the nucleus pulposus. PLoS ONE **9**: e110768. DOI:10.1371/journal.pone.0110768.

Mern DS, Beierfuß A, Thomé C, Hegewald AA (2014) Enhancing human nucleus pulposus cells for biological treatment approaches of degenerative intervertebral disc diseases: a systematic review. J Tissue Eng Regen Med **8**: 925-936. DOI: 10.1002/term.1583.

Minogue BM, Richardson SM, Zeef LAH, Freemont AJ, Hoyland JA (2010) Characterization of the human nucleus pulposus cell phenotype and evaluation of novel marker gene expression to define adult stem cell differentiation. Arthritis Rheum **62**: 3695-3705. DOI: 10.1002/art.27710.

Mohanty S, Dahia CL (2019) Defects in intervertebral disc and spine during development, degeneration, and pain: new research directions for disc regeneration and therapy. Wiley Interdiscip Rev Dev Biol **8**: e343. DOI: 10.1002/wdev.343.

Mohanty S, Pinelli R, Pricop P, Albert TJ, Dahia CL (2019) Chondrocyte-like nested cells in the aged intervertebral disc are late-stage nucleus pulposus cells. Aging Cell **18**: e13006. DOI: 10.1111/acel.13006.

Nguyen DT, Famiglietti JE, Smolchek RA, Dupee Z, Diodati N, Pedro DI, Urueña JM, Schaller MA, Sawyer WG (2022) 3D *In vitro* platform for cell and explant culture in liquid-like solids. Cells **11**: 967. DOI:10.3390/cells11060967.

Palacio-Mancheno PE, Evashwick-Rogler TW, Laudier DM, Purmessur D, Iatridis JC (2018) Hyperosmolarity induces notochordal cell differentiation with aquaporin3 upregulation and reduced N-cadherin expression. J Orthop Res **36**: 788-798. DOI: 10.1002/jor.23715.

Parton RG, del Pozo MA, Vassilopoulos S, Nabi IR, Le Lay S, Lundmark R, Kenworthy AK, Camus A, Blouin CM, Sessa WC, Lamaze C (2020) Caveolae: the FAQs. Traffic **21**: 181-185. DOI: 10.1111/tra.12689.

Pattappa G, Li Z, Peroglio M, Wismer N, Alini M, Grad S (2012) Diversity of intervertebral disc cells: phenotype and function. J Anat **221**: 480-496. DOI: 10.1111/j.1469-7580.2012.01521.x.

Peck SH, McKee KK, Tobias JW, Malhotra NR, Harfe BD, Smith LJ (2017) Whole transcriptome analysis of notochord-derived cells during embryonic formation of the nucleus pulposus. Sci Rep **7**: 10504. DOI: 10.1038/s41598-017-10692-5.

Potier E, de Vries S, van Doeselaar M, Ito K (2014) Potential application of notochordal cells for intervertebral disc regeneration: an *in vitro* assessment. Eur Cell Mater **28**: 68-80. DOI: 10.22203/ecm.v028a06.

Purmessur D, Guterl CC, Cho SK, Cornejo MC, Lam YW, Ballif BA, Laudier DM, Iatridis JC (2013) Dynamic pressurization induces transition of notochordal cells to a mature phenotype while retaining production of important patterning ligands from development. Arthritis Res Ther **15**: R122. DOI:10.1186/ar4302.

Rajesh D, Dahia CL (2018) Role of sonic hedgehog signaling pathway in intervertebral disk formation and maintenance. Curr Mol Biol Rep **4**: 173-179. DOI: 10.1007/s40610-018-0107-9.

Rajpurohit R, Risbud MV, Ducheyne P, Vresilovic EJ, Shapiro IM (2002) Phenotypic characteristics of the nucleus pulposus: expression of hypoxia inducing factor-1, glucose transporter-1 and MMP-2. Cell Tissue Res **308**: 401-407. DOI: 10.1007/s00441-002-0563-6.

Richardson SM, Knowles R, Marples D, Hoyland JA, Mobasheri A (2008) Aquaporin expression in the human intervertebral disc. J Mol Histol **39**: 303-309. DOI: 10.1007/s10735-008-9166-1.

Richardson SM, Ludwinski FE, Gnanalingham KK, Atkinson RA, Freemont AJ, Hoyland JA (2017) Notochordal and nucleus pulposus marker expression is maintained by sub-populations of adult human nucleus pulposus cells through aging and degeneration. Sci Rep **7**: 1501. DOI: 10.1038/s41598-017-01567-w.

Risbud MV, Schoepflin ZR, Mwale F, Kandel RA, Grad S, Iatridis JC, Sakai D, Hoyland JA (2015) Defining the phenotype of young healthy nucleus pulposus cells: recommendations of the spine research interest group at the 2014 annual ORS meeting. J Orthop Res **33**: 283-293. DOI: 10.1002/jor.22789.

Rodrigues-Pinto R, Berry A, Piper-Hanley K, Hanley N, Richardson SM, Hoyland JA (2016) Spatiotemporal analysis of putative notochordal cell markers reveals CD24 and keratins 8, 18, and 19 as notochord-specific markers during early human intervertebral disc development. J Orthop Res **34**: 1327-1340. DOI: 10.1002/jor.23205.

Rodrigues-Pinto R, Ward L, Humphreys M, Zeef LAH, Berry A, Hanley KP, Hanley N, Richardson SM, Hoyland JA (2018) Human notochordal cell transcriptome unveils potential regulators of cell function in the developing intervertebral disc. Sci Rep **8**: 12866. DOI:10.1038/s41598-018-31172-4.

Rosenzweig DH, Tremblay Gravel J, Bisson D, Ouellet JA, Weber MH, Haglund L (2017) Comparative analysis in continuous expansion of bovine and human primary nucleus pulposus cells for tissue repair applications. Eur Cell Mater **33**: 240-251. DOI: 10.22203/eCM.v033a18.

Sadowska A, Kameda T, Krupkova O, Wuertz-Kozak K (2018) Osmosensing, osmosignalling and inflammation: how intervertebral disc cells respond to altered osmolarity. Eur Cell Mater **36**: 231-250. DOI: 10.22203/eCM.v036a17.

Sedding DG, Hermsen J, Seay U, Eickelberg O, Kummer W, Schwencke C, Strasser RH, Tillmanns H, Braun-Dullaeus RC (2005) Caveolin-1 facilitates mechanosensitive protein kinase B (Akt) signaling *in vitro* and *in vivo*. Circ Res **96**: 635-642. DOI: 10.1161/01.RES.0000160610.61306.0f.

Séguin CA, Chan D, Dahia CL, Gazit Z (2018) Latest advances in intervertebral disc development and progenitor cells. JOR Spine **1**: e1030. DOI:10.1002/jsp2.1030.

Shamir ER, Ewald AJ (2014) Three-dimensional organotypic culture: experimental models of mammalian biology and disease. Nat Rev Mol Cell Biol **15**: 647-664. DOI: 10.1038/nrm3873.

Sinha B, Köster D, Ruez R, Gonnord P, Bastiani M, Abankwa D, Stan RV, Butler-Browne G, Vedie B, Johannes L, Morone N, Parton RG, Raposo G, Sens P, Lamaze C, Nassoy P (2011) Cells respond to mechanical stress by rapid disassembly of caveolae.

Cell **144**: 402-413. DOI: 10.1016/j.cell.2010.12.031.

Smith LJ, Nerurkar NL, Choi KS, Harfe BD, Elliott DM (2011) Degeneration and regeneration of the intervertebral disc: lessons from development. Dis Model Mech **4**: 31-41. DOI: 10.1242/dmm.006403.

Smolders LA, Meij BP, Onis D, Riemers FM, Bergknut N, Wubbolts R, Grinwis GCM, Houweling M, Groot Koerkamp MJA, van Leenen D, Holstege FCP, Hazewinkel HAW, Creemers LB, Penning LC, Tryfonidou MA (2013) Gene expression profiling of early intervertebral disc degeneration reveals a down-regulation of canonical Wnt signaling and caveolin-1 expression: implications for development of regenerative strategies. Arthritis Res Ther **15**: R23. DOI: 10.1186/ar4157.

Snuggs JW, Tessier S, Bunning RAB, Shapiro IM, Risbud MV, Le Maitre CL (2021) TonEBP regulates the hyperosmotic expression of aquaporin 1 and 5 in the intervertebral disc. Sci Rep **11**: 3164. DOI:10.1038/s41598-021-81838-9.

Snuggs JW, Day RE, Bach FC, Conner MT, Bunning RAD, Tryfonidou MA, Le Maitre CL (2019) Aquaporin expression in the human and canine intervertebral disc during maturation and degeneration. JOR Spine **2**: e1049. DOI: 10.1002/jsp2.1049.

Spillekom S, Smolders LA, Grinwis GCM, Arkesteijn ITM, Ito K, Meij BP, Tryfonidou MA (2014) Increased osmolarity and cell clustering preserve canine notochordal cell phenotype in culture. Tissue Eng Part C Methods **20**: 652-662. DOI: 10.1089/ten.TEC.2013.0479.

Stevens JW, Kurriger GL, Carter AS, Maynard JA (2000) CD44 expression in the developing and growing rat intervertebral disc. Dev Dyn **219**: 381-390. DOI: 10.1002/1097-0177(2000)9999:9999<::AID-DVDY1060>3.0.CO;2-P.

Tam V, Chan WCW, Leung VYL, Cheah KSE, Cheung KMC, Sakai D, McCann MR, Bedore J, Séguin CA, Chan D (2018) Histological and reference system for the analysis of mouse intervertebral disc. J Orthop Res **36**: 233-243. DOI: 10.1002/jor.23637.

Tang SN, Walter BA, Heimann MK, Gantt CC, Khan SN, Kokiko-Cochran ON, Askwith CC, Purmessur D (2022) *In vivo* mouse intervertebral disc degeneration models and their utility as translational models of clinical discogenic back pain: a comparative review. Front Pain Res (Lausanne) **3**. DOI:10.3389/fpain.2022.894651.

de Vries SAH, van Doeselaar M, Meij BP, Tryfonidou MA, Ito K (2018) Notochordal cell matrix: an inhibitor of neurite and blood vessel growth? J Orthop Res **36**: 3188-3195. DOI: 10.1002/jor.24114.

Wang F, Gao ZX, Cai F, Sinkemani A, Xie ZY, Shi R, Wei JN, Wu XT (2017) Formation, function, and exhaustion of notochordal cytoplasmic vacuoles within intervertebral disc: current understanding and speculation. Oncotarget **8**: 57800-57812. DOI: 10.18632/oncotarget.18101.

Williams RJ, Tryfonidou MA, Snuggs JW, Le Maitre CL (2021) Cell sources proposed for nucleus pulposus regeneration. JOR Spine **4**: e1175. DOI:10.1002/jsp2.1175.

Williams S, Alkhatib B, Serra R (2019) Development of the axial skeleton and intervertebral disc. Curr Top Dev Biol **133**: 49-90. DOI: 10.1016/bs.ctdb.2018.11.018.

Winkler T, Mahoney EJ, Sinner D, Wylie CC, Dahia CL (2014) Wnt signaling activates Shh signaling in early postnatal intervertebral discs, and re-activates Shh signaling in old discs in the mouse. PLoS One **9**: e98444. DOI:10.1371/journal.pone.0098444.

Wu A, March L, Zheng X, Huang J, Wang X, Zhao J, Blyth FM, Smith E, Buchbinder R, Hoy D (2020) Global low back pain prevalence and years lived with disability from 1990 to 2017: estimates from the Global Burden of Disease Study 2017. Ann Transl Med **8**: 299. DOI: 10.21037/atm.2020.02.175.

Discussion with Reviewer

Simon Tang: Congratulations to the authors for this outstanding work. This 3D model of notochordal cells will undoubtedly have a profound impact for scientists seeking to understand intervertebral disc biology. I wonder whether the authors could comment whether they envision these notochordal micromasses could differentiate into matrix-synthesising nucleus pulpous cells, even when challenged under the degenerative conditions of the IVD?

Authors: Absolutely, this suggestion is fully relevant as this 3D cell model system will allow the monitoring of notochordal cell behaviour in response to environmental changes, influencing cell signalling or cell-matrix interactions, or mediated through mechanical or osmolar stimuli, including the treatment with media mimicking degenerative environment developed by other scientists in the field of intervertebral disc biology.

Editor's note: The Scientific Editor responsible for this paper was Sibylle Grad.